Quantum dimer phases in a frustrated spin ladder: Effective field theory approach and exact diagonalization

Temo Vekua[1,2] and Andreas Honecker[3,4]
[1]*Laboratoire de Physique Théorique, Université Louis Pasteur, 67084 Strasbourg, France*
[2]*Andronikashvili Institute of Physics, Tamarashvili 6, 0177 Tbilisi, Georgia*
[3]*TU Braunschweig, Institut für Theoretische Physik, 38106 Braunschweig, Germany*
[4]*Institut für Theoretische Physik, Universität Göttingen, 37077 Göttingen, Germany*
(Received 24 January 2006; published 14 June 2006)

The phase diagram of a frustrated $S=1/2$ antiferromagnetic spin ladder with additional next-nearest neighbor exchanges, both diagonal and in-chain, is studied by a weak-coupling effective field theory approach combined with exact diagonalization for finite systems. In addition to two known phases with rung-singlet and Haldane-type ground states, we observe two new phases with dimerization along the chains. Furthermore, the transitions between the different phases are studied and shown to be either first order or to belong to the universality class of the two-dimensional Ising model. The nature of elementary excitations is discussed briefly.

DOI: 10.1103/PhysRevB.73.214427 PACS number(s): 75.10.Pq, 75.40.Cx, 75.30.Kz, 75.40.Mg

I. INTRODUCTION

During the past few decades, strongly correlated electron systems have received a lot of attention, e.g., due to unconventional superconductors. In particular, during the early days of high-T_c superconductivity, Anderson had already proposed a mechanism based on a so-called resonating valence-bond (RVB) picture.[1] Nevertheless, the search for a spin liquid in two dimensions remains a long-standing problem. In this context, much attention was devoted to the study of geometrically frustrated magnetic systems (for recent reviews see, e.g., Refs. 2 and 3).

Among the different proposed models to capture Anderson's RVB scenario is the one of Nersesyan and Tsvelik,[4] based on a spatially anisotropic J_1-J_2 square lattice with stronger exchanges along one particular "chain" direction to allow for generalizing results obtained previously in one dimension.[5] However, it turned out that even the one-dimensional picture was not completely under control:[6] in weak coupling it is impossible to fine-tune rung and diagonal exchanges of two-leg spin ladders to eliminate all relevant interchain couplings at all orders. In particular it was argued in Ref. 6 that at weak coupling there is no direct first-order phase transition from two phases with unique ground states, namely, a Haldane phase and a rung-singlet phase, rather an intermediate, spontaneously dimerized phase was predicted. However, previous numerical calculations have not detected this intermediate phase.[7] The numerically determined phase diagram suggested a direct phase transition from the Haldane to the rung-singlet phase which at weak interchain coupling seemed to be of second order and became first order at stronger couplings. While the latter topology of the phase diagram agrees with the earlier bosonization prediction,[5] the order of the phase transitions disagrees at weak coupling. We will argue that the intermediate phase in the spin ladder can be revealed by adding further exchanges.

In this work we study an $S=1/2$ antiferromagnetic two-leg spin ladder with additional next-nearest-neighbor exchanges and discuss the interplay between two distinct scales, one set by in-chain frustration and the other one by interchain interactions. In the spirit of Ref. 8, this model can also be regarded as a strip of the extensively studied J_1-J_2 -J_3 square lattice.[9,10] The last model illustrates that frustrated interactions in quantum spin systems give rise to "unpredictable" phases which are very difficult to analyze theoretically because of the presence of competing interactions. The study of the effect of additional next-nearest-neighbor exchanges in spin ladder systems therefore also is an interesting theoretical problem in its own right. The bosonization approach[11] is an unbiased and powerful method for studying frustrated systems in particular in one dimension. Using this method, we will show that a rich phase diagram and intriguing nature of elementary excitations result from the competing interactions in the frustrated spin ladder. Furthermore, numerical analysis of finite systems confirms the presence of the phases obtained within the weak-coupling effective field theory, also at larger couplings.

II. MODEL

We consider the $S=1/2$ antiferromagnetic Heisenberg spin ladder with additional next-nearest-neighbor exchanges which are represented by ladder diagonal and in-chain next-nearest-neighbor interactions. The geometry of our model is depicted in Fig. 1. The lattice Hamiltonian reads

$$\hat{H} = H^1_{leg} + H^2_{leg} + H_{int}, \tag{1}$$

where the Hamiltonian for leg $l=1,2$ is

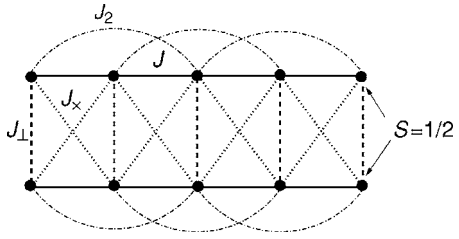

FIG. 1. Structure of the spin ladder with next-nearest-neighbor interactions.

$$H^l_{leg} = \sum_{j=1}^{N} (J\mathbf{S}_{l,j} \cdot \mathbf{S}_{l,j+1} + J_2 \mathbf{S}_{l,j} \cdot \mathbf{S}_{l,j+2}) \tag{2}$$

and the interleg coupling contains both the rung and the diagonal exchanges:

$$H_{int} = \sum_{j=1}^{N} [J_\perp \mathbf{S}_{1,j} \cdot \mathbf{S}_{2,j} + J_\times (\mathbf{S}_{1,j} \cdot \mathbf{S}_{2,j+1} + \mathbf{S}_{1,j+1} \cdot \mathbf{S}_{2,j})]. \tag{3}$$

Above, $\mathbf{S}_{l,j}$ represent spin $S=1/2$ operators on the jth rung and lth leg, and periodic boundary conditions are assumed, $\mathbf{S}_{l,N+1}=\mathbf{S}_{l,1}$. In order to avoid additional frustration by the boundary conditions, we will consider only even chain lengths N.

The above Hamiltonian (1) with $J_2=0$ has already been investigated in detail.[5,7,12,13] In particular the case $J_\times=J$, $J_2=0$ serves as a good illustration of two possible phases[12] since in this case the total spins on all rungs are good quantum numbers. Then the ground state consists of local singlets $S_{\text{rung}}=0$ for sufficiently large $J_\perp$ with a clear gap to all excitations. On the other hand, for small $J_\perp$, the total spin $S_{\text{rung}}=1$ is formed on each rung and the low-energy physics is governed by an effective spin-1 chain. In the latter case, the ground state is the famous Haldane state which is also gapped (see, e.g., Ref. 14 for a recent review of spin-chain models). These two phases extend to $J_\times \neq J$, $J_2 \neq 0$ and we refer to them as the rung-singlet and Haldane phases, respectively.

III. WEAK-COUPLING APPROACH, BOSONIZATION

In this section we perform the weak-coupling analysis of our system (1). We will follow the usual method and start from a continuous field theory description of the individual spin chain and treat the interchain interactions perturbatively.[11] We note that one can construct two equivalent weak-coupling formulations. One can start from decoupled chain limits where chains run either along the ladder legs, or along the ladder diagonals. These two cases are connected to each other by a duality transformation exchanging the spins on every second rung.[13] For definiteness we start from two decoupled frustrated chains running along the ladder legs: $J_\times, J_\perp \ll J$. Spin operators on each chain are decomposed into their smooth and staggered parts:

$$\frac{\mathbf{S}_{l,j}}{a_0} = \mathbf{S}_l(x = ja_0) = \mathbf{J}_l(x) + \bar{\mathbf{J}}_l(x) + (-1)^x \mathbf{n}_l(x) \tag{4}$$

with lattice constant a_0. $\mathbf{J}_l$ and $\bar{\mathbf{J}}_l$ are left and right SU(2) currents of the lth chain and have conformal weights (1,0) and (0,1), respectively. Staggered spin densities are represented by more relevant operators, indicating an inherent instability toward doubling of the unit cell in antiferromagnetic chains:

$$n^i_l(x) \sim \text{Tr}[\sigma^i g_l(x)]. \tag{5}$$

Here $g_l(x)$ stands for the basic 2×2 matrix field of the Wess-Zumino model and has conformal weights $(1/4, 1/4)$. σ^i are the Pauli matrices. The scalar quantity which is represented in the continuum limit by an operator of the same dimension as the staggered part of the magnetization is the dimerization operator:

$$\mathbf{S}_l(x)\mathbf{S}_l(x+a_0) = (-1)^x \epsilon_l(x) + (\text{less relevant smooth part}). \tag{6}$$

In terms of the basic Wess-Zumino matrix field the following representation holds for the dimerization operator:

$$\epsilon_l(x) \sim \text{Tr} g_l(x). \tag{7}$$

The effective quantum field theory in the continuum limit of a single chain is that of a critical $\text{SU}(2)_1$ Wess-Zumino model perturbed by a marginal current-current interaction:[15,16]

$$H_l = \frac{2\pi u}{3}(:\mathbf{J}_l\mathbf{J}_l: + :\bar{\mathbf{J}}_l\bar{\mathbf{J}}_l:) + \gamma \mathbf{J}_l\bar{\mathbf{J}}_l \tag{8}$$

with the following notations:

$$u = \frac{Ja_0\pi}{2} \quad \text{and} \quad \gamma = J_2 - J_{2,c},$$

where $J_{2,c} \simeq 0.24$.[17,18] If $\gamma<0$ the perturbation is marginally irrelevant, but when $\gamma>0$ the interaction flows toward strong coupling and the system dimerizes spontaneously with a dynamically generated gap in the excitation spectrum.[19] In Abelian bosonization representation we can rewrite Eq. (8) as

$$H_l = \frac{u}{2}\{[\theta_l(x)]^2 + [\partial_x \phi_l(x)]^2\} - \frac{\gamma}{2\pi^2} \cos\sqrt{8\pi}\phi_l + \frac{\gamma}{\pi}\partial_x\phi_{l,R}\partial_x\phi_{l,L} \tag{9}$$

with compactified dual bosonic fields θ and ϕ. The following representations hold for the staggered spin density and dimerization operators:[11]

$$\mathbf{n}_l(x) \sim (\cos\sqrt{2\pi}\theta_l(x), \sin\sqrt{2\pi}\theta_l(x), \sin\sqrt{2\pi}\phi_l(x)),$$

$$\epsilon_l(x) \sim \cos\sqrt{2\pi}\phi_l(x). \tag{10}$$

For further analyses, treating interchain coupling perturbatively, it will be convenient to pass to symmetric and antisymmetric combinations of the bosonic fields

$$\phi_\pm(x) = \frac{\phi_1(x) \pm \phi_2(x)}{\sqrt{2}} \tag{11}$$

and define the continuum limit expressions of order parameters for columnar and staggered dimerizations of the two chains:

$$\epsilon_+ = \epsilon_1 + \epsilon_2 \sim \cos\sqrt{\pi}\phi_+ \cos\sqrt{\pi}\phi_-,$$

$$\epsilon_- = \epsilon_1 - \epsilon_2 \sim \sin\sqrt{\pi}\phi_+ \sin\sqrt{\pi}\phi_-. \tag{12}$$

The Hamiltonian in the symmetric and antisymmetric sectors will contain a marginally relevant intersector coupling which promotes dimerization within the chains:

$$\frac{\gamma}{\pi}\partial_x\phi_{+,R}\partial_x\phi_{+,L}+\frac{\gamma}{\pi}\partial_x\phi_{-,R}\partial_x\phi_{-,L}$$

$$-\frac{\gamma}{\pi^2}\cos\sqrt{4\pi}\phi_+\cos\sqrt{4\pi}\phi_-. \quad (13)$$

The intersector interactions (13) show that the vacuum configurations of the symmetric and antisymmetric sectors are degenerate:

$$\langle\cos\sqrt{4\pi}\phi_+\rangle=\langle\cos\sqrt{4\pi}\phi_-\rangle=1 \quad \text{(a)},$$

$$\langle\cos\sqrt{4\pi}\phi_+\rangle=\langle\cos\sqrt{4\pi}\phi_-\rangle=-1 \quad \text{(b)}. \quad (14)$$

This includes the two-leg ladder dimerized in different patterns, namely, (a) with long-range ordered columnar and (b) with staggered dimerizations, respectively.

The expressions of spin operators in terms of the bosonic fields are valid as long as the dimerization is very weak. We can then add interchain interactions to the frustrated decoupled chains. We classify interchain couplings according to their scaling dimension:

$$H_{int}\sim(J_\perp+2J_\times)[\mathbf{J}_1(x)+\bar{\mathbf{J}}_1(x)][\mathbf{J}_2(x)+\bar{\mathbf{J}}_2(x)]+(J_\perp-2J_\times)\mathbf{n}_1(x)\mathbf{n}_2(x). \quad (15)$$

The product of the smooth parts of the spin operators is translated into marginal operators, whereas the product of the staggered parts is represented by relevant operators in the effective field theory.

A. Mean-field separation

As a first approximation and for $\gamma=0$, $J_\perp-2J_\times\neq0$, one can retain only relevant terms that stem from the product of the Néel components of the spin operators. In this case the effective field-theoretic Hamiltonian separates into two commuting parts in the symmetric and antisymmetric bases:[20,21]

$$H=H^+ + H^-,$$

$$H^+=\frac{u_+}{2}[(\partial_x\theta_+)^2+(\partial_x\phi_+)^2]-\frac{\tilde{J}_\perp c^2}{2\pi^2}\cos\sqrt{4\pi}\phi_+(x),$$

$$H^-=\frac{u_-}{2}\{(\partial_x\theta_-)^2+[\partial_x\phi_-(x)]^2\}+\frac{\tilde{J}_\perp c^2}{2\pi^2}\cos\sqrt{4\pi}\phi_-(x)+\frac{\tilde{J}_\perp c^2}{\pi^2}\cos\sqrt{4\pi}\theta_-(x), \quad (16)$$

where $\tilde{J}_\perp=J_\perp-2J_\times$, c stands for a nonuniversal numerical constant, and

$$u_\pm=u\left(1\pm\frac{\tilde{J}_\perp}{2\pi J}\right)$$

in weak coupling.

Now we add $\gamma>0$ and look at the limit $J_\perp,J_\times\ll\gamma\ll J$, which allows us to assume stability of the massive dimerized phases of the individual chains against infinetisimal interchain perturbation. For $J_\perp=J_\times=0$ the chains dimerize in columnar and staggered patterns, which corresponds to pinning of the symmetric and antisymmetric fields in degenerate vacua with nonzero averages of $\cos\sqrt{4\pi}\phi_\pm$. One may assume that these averages will be nonzero in a finite region of the parameter space after inclusion of interchain coupling such that we may substitute finite averages for $\cos\sqrt{4\pi}\phi_\pm$ in Eq. (13). In the antisymmetric sector the Hamiltonian density contains a relevant cosine of the bosonic field ϕ_- as well as its dual θ_- [see (16)]. By contrast, the dual field cannot appear in the symmetric sector for symmetry reasons. The classical vacuum configuration of the symmetric field is pinned unambiguously according to the sign of interchain coupling and thus any small interchain coupling (which is relevant) removes immediately the degeneracy of the ground state of decoupled dimerized chains (14). The picture is as follows. Addition of infinitesimally small relevant interchain coupling confines the massive spinons of the individual chains into magnons. At the same time, the ground-state degeneracy is lifted and one of the long-range-ordered dimerization patterns (columnar or staggered) is selected. Once the symmetric field ϕ_+ is pinned, we can perform a mean-field decoupling of the interaction term stemming from γ. Note that this procedure does not depend on the sign of $J_\perp-2J_\times\neq0$; the crucial assumption is that a relevant interchain coupling is present, which provides a confining potential to spinons of the individual dimerized chains and selects one of the two long-range-ordered dimerization patterns.

At the mean-field level we are left with the following Hamiltonian:

$$H_{MF}=H_0+\frac{\tilde{J}_\perp c^2}{\pi^2}\cos\sqrt{4\pi}\theta_-(x)-\left(\frac{\tilde{J}_\perp c^2}{2\pi^2}+\frac{\gamma}{\pi^2}\langle\cos\sqrt{4\pi}\phi_-(x)\rangle\right)\cos\sqrt{4\pi}\phi_+(x)+\left(\frac{\tilde{J}_\perp c^2}{2\pi^2}-\frac{\gamma}{\pi^2}\langle\cos\sqrt{4\pi}\phi_+(x)\rangle\right)\cos\sqrt{4\pi}\phi_-(x), \quad (17)$$

where H_0 stands for the sum of the Gaussian parts of the symmetric and antisymmetric sectors. This particular form of the mean-field Hamiltonian is convenient for passing to Majorana fermions, but let us first discuss artifacts of the mean-field separation: the mean-field separation in Eq. (17) breaks the underlying SU(2) symmetry of the ladder model to $U(1)\otimes\mathbb{Z}^2$. This is verified directly by noting that the very form of the mean-field Hamiltonian (17) coincides with the Hamiltonian of a ladder where the next-nearest in-chain frustrating coupling is substituted by the product of dimerization operators of the two chains and interchain coupling is of easy-plane type:

$$(A+B)\epsilon_1(x)\epsilon_2(x)+(A-B)n_1^zn_2^z \quad (18)$$

with

$$A = -\frac{\gamma}{\pi^2}\langle \cos\sqrt{4\pi}\phi_+(x)\rangle,$$

$$B = -\frac{\gamma}{\pi^2}\langle \cos\sqrt{4\pi}\phi_-(x)\rangle.$$

While the product of dimerization operators respects SU(2) symmetry, the appearance of an effective anisotropy in interchain coupling is clearly an artifact of the mean-field separation and should not be taken physically (e.g., splitting of the triplet of Majorana fermions into doublet and singlet). With increasing interchain exchange in Eq. (17) we observe a phase transition represented by a self-dual point in the antisymmetric sector:

$$\frac{\tilde{J}_\perp c^2}{2\pi^2} - \frac{\gamma}{\pi^2}\langle \cos\sqrt{4\pi}\phi_+(x)\rangle = -\frac{\tilde{J}_\perp c^2}{\pi^2}. \tag{19}$$

Since our approach is a weak-coupling one (starting from decoupled chains) we are dealing with a fixed-point Hamiltonian which is described in terms of two copies of the $SU(2)_1$ Wess-Zumino-Witten (WZW) model that is equivalent to an SO(4) WZW model. The SO(4) WZW model admits a representation of its generators in terms of four real Majorana fermions.[22] To clarify the symmetries of the stabilized dimerization pattern and to unveil the nature of the self-dual point in the antisymmetric sector we pass to these Majorana fermions and subsequently to Ising variables.

The mean-field Hamiltonian (17) takes the following form in Majorana fermions:[21]

$$H = -\int dx\left(\frac{iv_s}{2}(\rho_R\partial_x\rho_R - \rho_L\partial_x\rho_L) + im_s\rho_R\rho_L\right) - \sum_{a=1}^{3}\int dx\left(\frac{iv_t}{2}(\psi_R^a\partial_x\psi_R^a - \psi_L^a\partial_x\psi_L^a) + im_t\psi_R^a\psi_L^a\right) \tag{20}$$

where

$$m_t \approx (J_\perp - 2J_\times) + \mathrm{sgn}(J_\perp - 2J_\times)\tilde{\gamma},$$

$$m_s \approx -3(J_\perp - 2J_\times) + \mathrm{sgn}(J_\perp - 2J_\times)\tilde{\gamma} \tag{21}$$

and $\tilde{\gamma}\sim\exp(-2\pi/\gamma)>0$ in weak coupling. The appearance of the sign function in the expressions for the masses of the Majorana fermions is the most important result of the mean-field treatment. Equation (21) shows that only the singlet among the Majorana fermions can soften by varying interchain interactions. Note that the triplet and singlet Majorana fermions can be interpreted as follows in the limit of strong rung coupling: the triplet ψ^a corresponds to a rung magnon (a triplet excitation on a rung), while the singlet ρ corresponds to the singlet bound state of two magnons. Indeed, we will argue soon that in the context of the effective field theory the singlet Majorana fermion softens at Ising phase transitions. On the other hand, we will show in Sec. IV C that the same Ising phase transitions can be traced to the softening of a singlet bound state of two magnons in our exact diagonalization data.

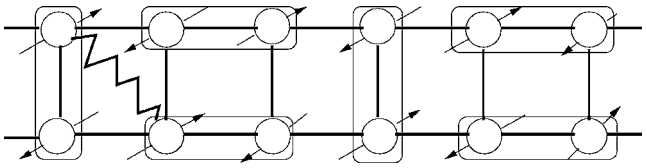

FIG. 2. Typical configuration in the RVB state of the antiferromagnetic ladder.

It is well known that a Majorana fermion describes the long-distance properties of the two-dimensional Ising model,[23] with the mass of the fermion proportional to the deviation from criticality $m\sim(T-T_c)/T_c$, meaning in particular that positive mass corresponds to the disordered phase of the Ising model. The following local representations hold in Ising variables for the order parameters of the columnar and staggered dimerized phases $\epsilon_\pm$:[11,21]

$$\epsilon_+ \sim \mu_1\mu_2\mu_3\mu_4, \quad \epsilon_- \sim \sigma_1\sigma_2\sigma_3\sigma_4, \tag{22}$$

where μ_i and σ_i are disorder and order variables of the ith replica of the two-dimensional Ising model, respectively.[24]

From the above formulas we read off the following picture. If we add to decoupled dimerized chains a relevant coupling with positive relevant exchange, $J_\perp - 2J_\times > 0$, then four copies of the Ising model will be in the disordered state, meaning that the ground state will have columnar dimer order. In the case of $J_\perp - 2J_\times < 0$, a staggered dimerized ground state will be selected. This analysis is supported by the following topological arguments: the ground state of the ordinary antiferromagnetic ladder is parity symmetric, $\langle\epsilon_\pm\rangle = 0$. A typical configuration in the resonating-valence-bond state of the antiferromagnetic ladder is depicted in Fig. 2, with rectangular boxes indicating singlets formed between the nearest-neighbor spins and the zigzag line representing an effective $S=1$ spin formed across the ladder diagonal.

One can introduce even and odd topological ("string") order parameters, as described in Refs. 25 and 26. These string order parameters have a simple geometric interpretation: they count the number of valence bonds crossed by an arbitrary vertical line such that the even string order parameter is nonzero if the number of crossed bonds is even and the odd one is nonzero if this number is odd. A nice feature of the two-leg ladder systems is that short-range valence-bond configurations have definite parity string order parameter.[26]

In the rung-singlet phase the even string order parameter is nonzero. Since γ does not introduce coupling between the chains both patterns of dimerization (columnar and staggered) are energetically equally favorable at this level, and from Fig. 2 it is clear that the columnar dimer configuration will be long-range ordered after adding relevant interchain coupling with $J_\perp - 2J_\times > 0$. Similar arguments apply to the case $J_\perp - 2J_\times < 0$. From the topology of typical configurations of the RVB state one can see in this case that singlets formed along the ladder diagonals coexist with staggered dimer configurations.[25,27] The string order parameter is odd and upon increasing inchain frustration the staggered dimer phase will be selected for the ground state. Crossing the sur-

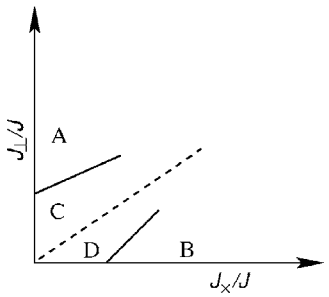

FIG. 3. Topology of the phase diagram as captured within the weak-coupling approach. Phases are as follows. A, rung singlet, B, Haldane, C, columnar dimer, and D, staggered dimer. The dashed line represents a first-order phase transition line, whereas continuous lines stand for Ising transition lines. Deviations of the dashed line at weak coupling from the straight line $J_\perp=2J_\times$ and enlargement of the columnar dimer phase are due to second-order processes as found in Ref. 6.

face which at weak couplings reads $J_\perp-2J_\times\sim 0$, the string order parameter jumps from even to odd by a first-order phase transition. These findings are summarized by the qualitative weak-coupling phase diagram Fig. 3.

Equation (21) also shows that gaps open linearly as one deviates from the Ising transition lines either in the rung-singlet or in the Haldane phase direction.

Let us summarize the mean-field scenario presented above and the supporting topological arguments: when two dimerized chains are coupled in such a way that relevant interchain coupling is present (in the model which we consider it is always present at weak couplings[6]) it provides a confining potential between the gapped spinons of the individual chains and the fourfold degeneracy of the ground state is reduced to twofold. But what can we say when interchain coupling is itself frustrated, i.e., when no relevant terms stem from interchain exchange and no confining potential is supplied for deconfined gapped spinons (for example, if we add additional four-spin interactions)? We answer these issues in the next section where we derive the quantum phase transition when both competing interactions (in chain as well as interchain) are marginal.

B. Mapping to the Gross-Neveu model

In this section we fine-tune interchain exchange to cancel relevant contributions. As recently discussed by Starykh *et al.*,[6] in the simple model (1) interchain exchange cannot be fine tuned to yield only marginal interactions unless we add four-spin counterterms.[28] In real systems small four-spin interactions are always present, e.g., represented by the cyclic ring exchange. So we can assume that we start from the line $J_\perp-2J_\times=0$ and relevant terms generated in second order are compensated with small four-spin counterterms. In that case the low-energy degrees of freedom of our fine-tuned model will be described by the triplet and singlet massless Majorana fermions coupled by marginal four-Fermi interactions alone:

$$H_{\mathrm{marg}}=Ja_0\int dx[(\lambda+\gamma)\times(\psi_R^1\psi_L^1\psi_R^2\psi_L^2+\psi_R^2\psi_L^2\psi_R^3\psi_L^3+\psi_R^1\psi_L^1\psi_R^3\psi_L^3)-(\lambda-\gamma)(\psi_R^1\psi_L^1+\psi_R^2\psi_L^2+\psi_R^3\psi_L^3)\rho_R\rho_L], \quad (23)$$

where $\lambda=J_\perp+2J_\times=2J_\perp$. As long as $\gamma<\lambda$, including negative γ, we can repeat the analysis by Allen *et al.*[5] where neglecting the anisotropy a mapping to the O(4) Gross-Neveu model[29] was used. Based on the one-loop renormalization group equations one can check that negative γ flows to zero at low energies and neglecting the anisotropy will not affect the ground-state properties of the model, neither will the excitation spectrum be modified qualitatively. On increasing γ to zero the mapping to the O(4) Gross-Neveu model becomes only a better approximation and exactly when $\gamma=0$ the O(4) Gross-Neveu model is the exact low-energy effective field theory describing chains coupled by frustrated interchain interaction. On further increasing in-chain frustration, telescoping (23) shows that at the point where

$$\gamma=\lambda=2J_\perp \quad (24)$$

a further quantum phase transition takes place where the zeroth Majorana fermion decouples from the rest of the triplet. Low-energy excitations at this quantum critical point are governed by a free massless Majorana fermion plus an O(3) Gross-Neveu model with dynamically generated mass for the remaining triplet of Majorana fermions. In the extreme limit $\gamma\gg\lambda$ we can neglect the small anisotropy between triplet and singlet Majorana fermions and recover the O(4)-invariant Gross-Neveu model, with dynamically generated mass. The sign of the mass defines the dimerization pattern of the model. Elementary excitations are deconfined massive spinons which interpolate between the fourfold degenerate vacua of the lattice model. This theory describes a first-order phase transition line between the columnar dimer and staggered dimer phases.

IV. NUMERICAL RESULTS

In order to test numerically the predictions for the phase diagram and the nature of phase transitions we start from the Majumdar-Ghosh point $J_2=J/2$ in the decoupled chains.[30] Each of the decoupled chains then has two degenerate dimerized ground states with a gap to the excitations. This behavior is generic in the vicinity of the Majumdar-Ghosh point, but the correlation length is minimal exactly at $J_2=J/2$.[31] Such a short correlation length is advantageous for numerical calculations since it minimizes finite-size effects.

For two weakly coupled dimerized chains, there will be four states that are well separated from higher excitations. We then need to clarify which ground state is formed depending on the coupling between the chains. In this context, it is interesting to note that for the particular choice $J_\perp=2J_\times$ of interchain coupling at $J_2=J/2$, the two staggered dimer arrangements remain exact eigenstates. Indeed, it is straightforward to check that interchain coupling terms cancel on the staggered dimer states. On the other hand, colum-

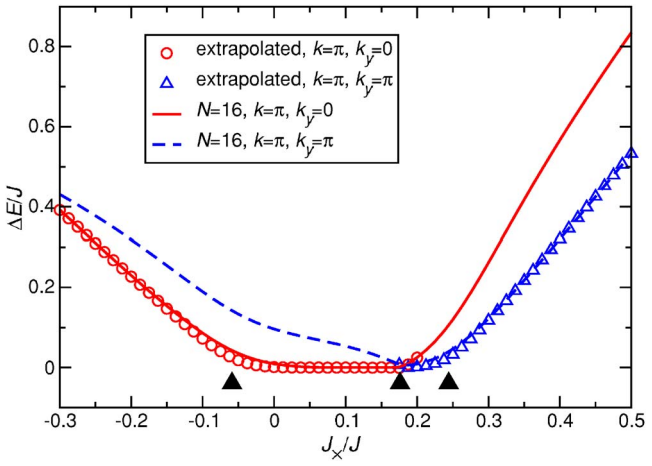

FIG. 4. (Color online) Numerical results for the lowest excited states with $S=0$ and $k=\pi$ at $J_2=J/2$, $J_\perp=0.2J$ as a function of $J_\times$. Lines are for $N=16$ rungs; symbols show extrapolations to the thermodynamic limit. The big filled triangles denote estimates for the locations of the different phase transitions. For details see the text.

nar dimer states cease to be exact eigenstates of the full ladder Hamiltonian; thus they can lower their energy by fluctuations. Therefore, we expect that two chains with $J_2=J/2$ weakly coupled by $J_\perp=2J_\times$ will have a columnar dimer pattern in the ground state.

To determine the ground-state phase diagram, we have performed exact diagonalization of ladders with up to $N=16$ rungs (32 spins) using a standard Lanczos method, exploiting the conservation of total S^z and spatial symmetries. We impose periodic boundary conditions along the chains in order to have translational symmetry. Furthermore, there is an exchange symmetry of the chains. Important information about the ground state is provided by the associated quantum numbers, in particular momentum k for translation along the chains, and k_y for the "momentum" corresponding to an exchange of the chains. On a finite system, the two staggered and columnar dimer states both combine to a ground state with $k=0$, $k_y=0$. However, the value of k_y in the first excited state distinguishes between the two cases: a combination of staggered dimer states gives rise to $k=\pi$, $k_y=\pi$, while one obtains $k=\pi$, $k_y=0$ from the columnar dimer states.

Extrapolations to the thermodynamic limit $N\to\infty$ will be performed using the Vanden-Broeck-Schwartz (VBS) algorithm[32,33] (with the parameter $\alpha=-1$ of the algorithm).

A. Low-lying levels

To illustrate the generic behavior, we will first discuss a cut through the phase diagram at $J_\perp=0.2J$. The lines in Fig. 4 show the excitation energy relative to the ground state for the lowest levels with $k=\pi$, $k_y=0$ and π on a finite system with $N=16$ rungs. On the left side of Fig. 4, all excitations are gapped, consistent with a rung-singlet phase. For $0\lesssim J_\times\lesssim 0.18J$, the $k=\pi$, $k_y=0$ level approaches the ground state, as is expected in a columnar dimer phase. Note that the point $J_\perp=0.2J$, $J_\times=0.1J$ lies inside the columnar dimer phase, as is expected since it belongs to the line $J_\perp=2J_\times$ discussed above. On the other hand, for $J_\times\approx 0.2J$, it is the level with $k=\pi$, $k_y=\pi$ which is approaching the ground state. This behavior is consistent with a staggered dimer phase around $J_\times\approx 0.2J$. Finally, on the right side of Fig. 4, all excitations are again gapped, consistent with a Haldane phase.

The locations of the phase transitions shown by the three big filled triangles in Fig. 4 are determined as follows. For intermediate $J_\times$, the levels shown in Fig. 4 are the only low-lying excitations, implying a direct first-order transition from the columnar dimer to the staggered dimer phase. We take the crossing of these two excited levels on a ladder with N rungs as an estimate for the transition point. We then extrapolate the crossing points with $6\leqslant N\leqslant 16$ rungs using the VBS algorithm. This extrapolation leads to the middle triangle in Fig. 4. Since the dependence on N is only weak, this extrapolated point is very close to the finite-size estimate for $N=16$.

The transitions to the rung-singlet phase and the Haldane phase at the left and right boundaries are expected to be second-order phase transitions. Such transitions can be accurately estimated using the phenomenological renormalization group method:[34] The critical couplings $\{J\}$ are determined by the condition that the levels for two different system sizes N_1, N_2 satisfy

$$N_1\Delta E_{k=\pi,k_y}(N_1,\{J\}) = N_2\Delta E_{k=\pi,k_y}(N_2,\{J\}). \qquad (25)$$

Here, one should choose $k_y=0$ and π for the transitions into the columnar and staggered dimer phases, respectively. Application of (25) to $N_1=14$ and $N_2=16$ yields the two remaining filled triangles in Fig. 4 (we neglect the dependence on N_1 and N_2 since in this case it is only weak).

Finally, the open circles and triangles in Fig. 4 show an extrapolation to the thermodynamic limits of the $k_y=0$ and the $k_y=\pi$ levels, respectively. This extrapolation has been performed with system sizes starting at $N=4$ rungs using the VBS algorithm. Errors of the extrapolation are difficult to estimate, but should not exceed the size of the symbols. In some cases, no convergence can be seen in the finite-size data for the higher-lying level such that no extrapolation can be performed for that level. However, in these regions of $J_\times$, the energy of the higher level shows a tendency to increase with N for the accessible system sizes. Thus, the higher-lying level can safely be assumed to stay at high energies in those regions where we cannot extrapolate it.

The behavior of the extrapolated gaps is essentially linear approaching the two second-order phase transitions from the outside. This is consistent with a critical exponent $\nu=1$, characteristic of the two-dimensional Ising universality class[35,36] predicted above.

B. Phase diagram

Now we apply the results of the preceding subsection to determine the full phase diagram for $0\leqslant J_\times\leqslant J$, $0\leqslant J_\perp$ in the plane $J_2=J/2$. Numerical scans were performed for $N\leqslant 14$ rungs since they require diagonalizations for a large set of data points (we have performed computations for approximately 4000 different pairs of $J_\times$ and $J_\perp$ at $N=14$). In se-

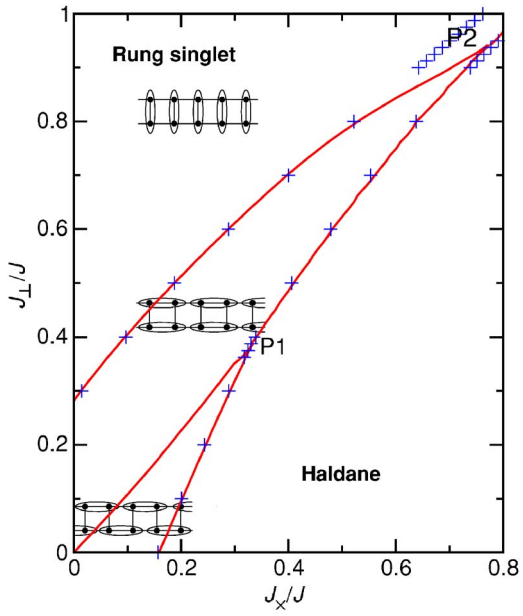

FIG. 5. (Color online) Numerical results for the phase diagram in the $J_2=J/2$ plane. Rung-singlet, Haldane, columnar dimer, and staggered dimer phases can be distinguished. Crosses have been determined by the phenomenological renormalization group condition (25) with $N_1=14$, $N_2=16$; the corresponding lines with $N_1=12$, $N_2=14$. For further details and the nature of the phase transitions see the text.

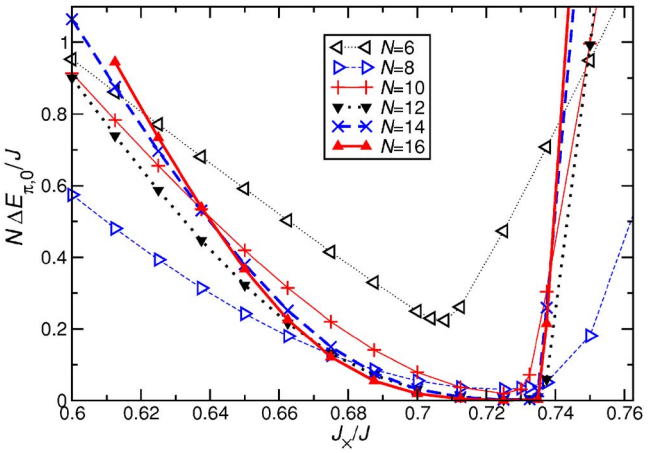

FIG. 6. (Color online) Scaled energies of the $k=\pi$, $k_y=0$ excited level for $J_\perp=0.9J$, $J_2=J/2$ as a function of $J_\times$. Lines connect actual numerical results, which are shown by symbols. According to the phenomenological renormalization group condition (25), crossings of levels for different N are estimates for the boundaries of the columnar dimer phase.

lected regions we performed additional computations for $N=16$. Figure 5 summarizes our results. One can distinguish four different gapped phases. A rung-singlet and a Haldane phase appear at large $J_\perp$ and $J_\times$, respectively. Previous results[8] for the point $J_\times=0$, $J_\perp=J$, $J_2=J/2$ are consistent with our conclusion that this lies well inside the rung-singlet. The rung-singlet and the Haldane phase phases have a nondegenerate ground state for a system with periodic boundary conditions. Between these two phases there exist two dimerized phases for small values of $J_\times$ and $J_\perp$, namely, a staggered and a columnar dimer phase. The latter phases have a twofold degenerate ground state with a spontaneously broken translational symmetry in the thermodynamic limit $N\to\infty$.

The transition between the staggered and columnar dimer phases is of first order and was determined as described in Sec. IV A: level crossings were first determined for fixed $6\leqslant N\leqslant 14$ (16 close to P1) and then extrapolated to $N\to\infty$ using the VBS algorithm. The error of this extrapolation is at most on the order of the width of the line. This transition line passes through the origin, as is expected by consideration of two decoupled dimerized chains.

The transitions from the dimerized phases to the rung-singlet or Haldane phases were determined by the phenomenological renormalization group method (25) with $N_1=12$, $N_2=14$ (lines) and $N_1=14$, $N_2=16$ (crosses). This is certainly justified for the transition between the columnar dimer and rung-singlet phases as well as the transition between the staggered dimer and Haldane phases, since these should be second-order transitions belonging to the two-dimensional Ising universality class. The transition between the columnar dimer and Haldane phases was also estimated by the phenomenological renormalization group method, although this may actually be a first-order transition. Nevertheless, finite-size effects are small (see, e.g., right side of Fig. 6). Therefore, our estimates for the transition between the columnar dimer and Haldane phases are probably quite accurate, even if we may not have used the most appropriate method.

The intermediate dimerized phases disappear (at least according to the $N_1=12$, $N_2=14$ estimates) for large interchain couplings at points P1 and P2, respectively. Beyond the point P2, one expects a direct first-order transition from the Haldane to the rung-singlet phase, as in the case $J_2=0$.[7,12] As in Ref. 7, we determine the location of this first-order transition from a cusp in the ground-state energy, using the data for $N=14$ rungs. The transitions between the rung-singlet and Haldane phases at $J_2=0$ and $J_2=J/2$ probably belong to the same universal surface of first-order transitions.

Finite-size effects of the transition lines are small in most regions of Fig. 5, as can be seen by comparison of the results for $N_1=12$, $N_2=14$ and $N_1=14$, $N_2=16$. This applies in particular to the neighborhood of P1 whose location can therefore be considered accurate. However, close to P2, we observe finite-size effects of the boundaries of the columnar dimer phase. In order to discuss this in more detail, Fig. 6 shows scaled energies of the $k=\pi$, $k_y=0$ excited level for $J_\perp=0.9J$, $J_2=J/2$, and $6\leqslant N\leqslant 16$. The crossings between the scaled levels for different N estimate the phase boundaries according to the phenomenological renormalization group condition (25). Unfortunately there is no systematic dependence of the crossings points on N_1,N_2 such that an extrapolation is not possible. Most crossings for the transition to the rung-singlet phase (left side of Fig. 6) lie between the $N_1=14$, $N_2=16$ crossing at $J_\times\approx 0.642J$ and the $N_1=12$, $N_2=14$ crossing at $J_\times\approx 0.704J$. Furthermore, linear extrapolation of the levels for fixed N suggests a closing of the gap and thus a phase transition around $J_\times\approx 0.66J$. Overall, it seems likely that the $N_1=12$, $N_2=14$ data underestimate the stability region of the columnar dimer phase, while $N_1=14$,

$N_2=16$ may overestimate it. Thus, the location of the termination point P2 is probably at larger $J_\times, J_\perp$ in the thermodynamic limit than the estimate in Fig. 5. Still one can argue that the columnar dimer phase has to terminate. First, it cannot extend beyond $J_\times=J$, since the duality transformation mentioned at the beginning of Sec. III maps the columnar dimer phase which we observe for $J_\times<J$ to a different phase with dimers on the diagonals for $J'_\times=J>J'=J_\times$, $J'_\perp=J_\perp$. Second, the region where $J_\perp$ is much bigger than all other exchange constants obviously belongs to the rung-singlet phase.[37] Therefore, the columnar dimer phase has to terminate either at a point P2 located in the region $J_\times<J$, or on the line $J_\times=J$. If the latter situation is realized we cannot exclude the possibility that the rung-singlet and Haldane phases are separated by a Gaussian quantum critical point located at $J_\times=J$.

Finally, we discuss the relation of the numerical phase diagram to the picture obtained by the mapping to the Gross-Neveu model presented in Sec. III B. Numerically we see that the columnar dimer phase extends to stronger interchain couplings than the staggered dimer phase. This gives further support to the observation that additional interactions such as ring exchange are necessary to fine-tune all relevant interchain couplings to zero. Indeed, it was found that ring exchange stabilizes staggered dimer order.[38,39] Therefore, ring exchange will cause the points P1 and P2 in Fig. 5 to move toward each other. P1 and P2 will merge when all relevant interchain couplings are fine tuned to zero. For the latter situation the effective theory of the multicritical point will be described by one gapless Majorana fermion decoupled from the rest of the gapped O(3) Gross-Neveu model as presented in Sec. III B. Since the effective field theory describing long-wavelength fluctuations of our model has a form similar to the one considered in Ref. 6, the same conclusion concerning the need to include additional four-spin interactions in order to suppress all relevant interchain couplings applies to the case $J_2=0$ considered in Ref. 6.

C. Softening of a bound state

In this last section we will comment on the nature of the elementary excitations. For this purpose we start from strong $J_\perp$ where one naturally obtains a rung-singlet phase[37] and approach the transition to the columnar dimer phase along the line $J_\times=0$. Since we just wish to make a qualitative point, we restrict ourselves to $N=12$ rungs in this section. Figure 7 shows numerical results at $J_\times=0$, $J_2=J/2$ for the lowest excited levels in the sectors with total spin $S=0$, 1, and 2. At strong $J_\perp$ the lowest excitation is a propagating triplet around $\Delta E=J_\perp$ above a nondegenerate ground state. On the other hand, the singlet excitation which softens at the transition to a columnar dimer state at $J_\perp\approx 0.29J$ can be traced to the lower boundary the $S=2$ continuum which starts at $\Delta E=2J_\perp$ for $J_\perp\to\infty$. This implies that the singlet which at small $J_\perp$ is a low-energy excitation originates from a bound state of two triplets at strong $J_\perp$. For the parameters of Fig. 7, this bound state has lower energy than the fundamental triplet for $J_\perp\lesssim 0.8J$ and finally softens at the Ising transition while states with nonzero total spin remain at a finite energy.

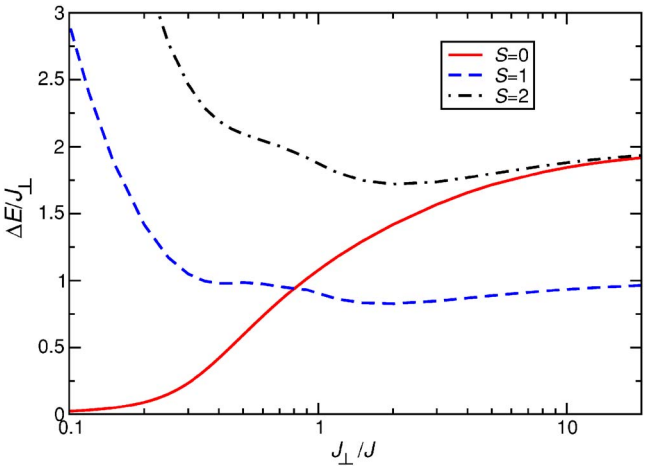

FIG. 7. (Color online) The lowest excited levels with total spin $S=0$, 1, and 2 on a ladder with $N=12$ rungs for $J_\times=0$, $J_2=J/2$ as a function of $J_\perp$ on a semilogarithmic scale.

Similarly, the transition from the Haldane phase to the staggered dimer phase should occur via softening of an $S=0$ two-magnon bound state while a single magnon remains gapped at the transition.

It is straightforward to analyze the one triplet and the bound-state problem of two triplets by perturbation theory at strong $J_\perp$. In fact, formation of bound states has been observed for ladders with $J_2=J_\times=0$ (see, e.g., Ref. 40). However, in this case none of the bound states has lower energy than the lowest edge of the two-triplet continuum. Two things happen when one turns on J_2 or $J_\times$. First, the minimum of the single-triplet dispersion generally shifts to incommensurate wave vectors. Second, now a bound state can appear at strong coupling which has an energy below the lowest edge of the two-particle continuum (see also Ref. 41 for $J_2=0$). However, it is necessary to go to high orders[42] to obtain quantitative agreement with numerical data. Therefore we do not pursue this further here.

Finally, we would like to mention that the bound-state nature of the lowest excitation leads to unusual finite-size effects close to the phase transitions and thus explains the difficulties with the extrapolations encountered in the previous subsections.

V. CONCLUSIONS

We have studied the ground-state phase diagram and the nature of elementary excitations of a frustrated spin ladder. The effect of relevant and marginal interchain exchanges has been analyzed by an effective field theory approach. Particular attention was paid to the interplay between two clearly separate scales set by in-chain frustration and interchain couplings. First, a rung-singlet and a Haldane phase are known to appear for $J_2=0$.[5,7,12,13,41] We predicted that for sufficiently large J_2, two dimerized phases appear between the rung-singlet and Haldane phases. The transitions from the dimerized phases to the rung-singlet and Haldane phases are found to be in the two-dimensional Ising universality class, whereas the transition between the columnar and staggered dimer phases is of first order.

Furthermore, we have verified these predictions by exact diagonalization. The full phase diagram has been determined in the plane $J_2=J/2$ (see Fig. 5). The staggered dimer phase was found to terminate first at a point P1 while the columnar dimer phase extends to stronger interchain coupling, terminating at P2. Beyond P2 there is a direct first-order transition from the rung-singlet to the Haldane phase if P2 is located at $J_\times<J$, as for $J_2=0$.[7,12] Should P2 be located at $J_\times=J$,[43] the rung-singlet and Haldane phases might be separated by a second-order phase transition point.

The part of the phase diagram with $J_\times>J$ is obtained from the one with $J_\times<J$ by a duality-type argument.[13] In particular, the columnar and staggered dimer phases map to two different dimerized phases with dimers on the diagonals.

Finally, we have observed an interesting phenomenon when approaching the columnar or staggered dimer phase from the rung-singlet or Haldane phase, respectively; namely, a singlet bound state forms below the two-triplet scattering continuum. This singlet bound state crosses the fundamental triplet excitation and finally softens at the Ising phase transition.

Since all phases are gapped, they will be stable under weak higher-dimensional coupling between the ladders. If one approaches the J_1-J_2-J_3 frustrated square lattice[9,10] by such interladder coupling, the rung-singlet phase will be adjacent to a Néel phase, and the Haldane phase will share a boundary with a phase where spins are ordered antiferromagnetically along one ladder direction and ferromagnetically along the other direction. Our results show that in such a generalized phase diagram there will be further dimerized phases, in particular some with two-dimensional columnar and staggered dimer patterns. We therefore hope that our results will also be useful to elucidate the phase diagram of the J_1-J_2-J_3 frustrated spin-1/2 Heisenberg antiferromagnet on the square lattice.[9,10]

ACKNOWLEDGMENTS

This work was initiated at the Institut für Theoretische Physik (ITP), University of Hannover. Both authors would like to thank the ITP for the hospitality extended to them during this period. We are particularly grateful to H.-J. Mikeska for valuable discussions. Furthermore, A.H. would like to acknowledge the Laboratoire de Physique Théorique, ULP Strasbourg for hospitality during the final stages of this work. Parts of the numerical computations have been performed on COMPAQ ES45 and SGI Altix 350 compute servers at the TU Braunschweig and ULP Strasbourg, respectively.

[1] P. W. Anderson, Science **235**, 1196 (1987).
[2] G. Misguich and C. Lhuillier, in *Frustrated Spin Systems*, edited by H. T. Diep (World Scientific, Singapore, 2005).
[3] J. Richter, J. Schulenburg, and A. Honecker, Lect. Notes Phys. **645**, 85 (2004).
[4] A. A. Nersesyan and A. M. Tsvelik, Phys. Rev. B **67**, 024422 (2003).
[5] D. Allen, F. H. L. Essler, and A. A. Nersesyan, Phys. Rev. B **61**, 8871 (2000).
[6] O. A. Starykh and L. Balents, Phys. Rev. Lett. **93**, 127202 (2004).
[7] X. Wang, Mod. Phys. Lett. B **14**, 327 (2000).
[8] L. Capriotti, D. J. Scalapino, and S. R. White, Phys. Rev. Lett. **93**, 177004 (2004).
[9] S. Sachdev and R. N. Bhatt, Phys. Rev. B **41**, 9323 (1990); A. Chubukov, *ibid.* **44**, 392 (1991); I. G. Gochev, *ibid.* **51**, 16421 (1995); L. Capriotti and S. Sachdev, Phys. Rev. Lett. **93**, 257206 (2004).
[10] M. P. Gelfand, R. R. P. Singh, and D. A. Huse, Phys. Rev. B **40**, 10801 (1989); P. W. Leung and N. W. Lam, *ibid.* **53**, 2213 (1996).
[11] A. O. Gogolin, A. A. Nersesyan, and A. M. Tsvelik, *Bosonization and Strongly Correlated Systems* (Cambridge University Press, Cambridge, U.K., 1999).
[12] M. P. Gelfand, Phys. Rev. B **43**, 8644 (1991); I. Bose and S. Gayen, *ibid.* **48**, 10653 (1993); Y. Xian, *ibid.* **52**, 12485 (1995); H. Kitatani and T. Oguchi, J. Phys. Soc. Jpn. **65**, 1387 (1996); A. Honecker, F. Mila, and M. Troyer, Eur. Phys. J. B **15**, 227 (2000).
[13] Zheng Weihong, V. Kotov, and J. Oitmaa, Phys. Rev. B **57**, 11439 (1998).
[14] H.-J. Mikeska and A. K. Kolezhuk, Lect. Notes Phys. **645**, 1 (2004).
[15] I. Affleck, in *Fields, Strings and Critical Phenomena*, edited by E. Brézin and J. Zinn-Justin (Elsevier, Amsterdam, 1990).
[16] D. C. Cabra and P. Pujol, Lect. Notes Phys. **645**, 253 (2004).
[17] K. Okamoto and K. Nomura, Phys. Lett. A **169**, 433 (1992).
[18] S. Eggert, Phys. Rev. B **54**, R9612 (1996).
[19] F. D. M. Haldane, Phys. Rev. B **25**, R4925 (1982).
[20] K. Totsuka and M. Suzuki, J. Phys.: Condens. Matter **7**, 6079 (1995).
[21] D. G. Shelton, A. A. Nersesyan, and A. M. Tsvelik, Phys. Rev. B **53**, 8521 (1996).
[22] D. Allen and D. Sénéchal, Phys. Rev. B **55**, 299 (1997).
[23] C. Itzykson and J.-M. Drouffe, *Statistical Field Theory* (Cambridge University Press, Cambridge, U.K., 1989), Vol. 1.
[24] L. P. Kadanoff and H. Ceva, Phys. Rev. B **3**, 3918 (1971).
[25] S. R. White, Phys. Rev. B **53**, 52 (1996).
[26] E. H. Kim, G. Fáth, J. Sólyom, and D. J. Scalapino, Phys. Rev. B **62**, 14965 (2000).
[27] S. R. White, R. M. Noack, and D. J. Scalapino, Phys. Rev. Lett. **73**, 886 (1994).
[28] A. M. Tsvelik, Phys. Rev. B **70**, 134412 (2004).
[29] D. Gross and A. Neveu, Phys. Rev. D **10**, 3235 (1974).
[30] C. K. Majumdar and D. K. Ghosh, J. Math. Phys. **10**, 1399 (1969).
[31] S. R. White and I. Affleck, Phys. Rev. B **54**, 9862 (1996).
[32] J.-M. vanden Broeck and L. W. Schwartz, SIAM J. Math. Anal. **10**, 658 (1979).
[33] M. Henkel and G. Schütz, J. Phys. A **21**, 2617 (1988).
[34] H. H. Roomany and H. W. Wyld, Phys. Rev. D **21**, 3341 (1980).

[35] L. Onsager, Phys. Rev. **65**, 117 (1944).
[36] M. E. Fisher and R. J. Burford, Phys. Rev. **156**, 583 (1967).
[37] T. Barnes, E. Dagotto, J. Riera, and E. S. Swanson, Phys. Rev. B **47**, 3196 (1993).
[38] M. Müller, T. Vekua, and H.-J. Mikeska, Phys. Rev. B **66**, 134423 (2002).
[39] A. Läuchli, G. Schmid, and M. Troyer, Phys. Rev. B **67**, 100409(R) (2003).
[40] O. P. Sushkov and V. N. Kotov, Phys. Rev. Lett. **81**, 1941 (1998).
[41] V. N. Kotov, O. P. Sushkov, and R. Eder, Phys. Rev. B **59**, 6266 (1999).
[42] S. Trebst, H. Monien, C. J. Hamer, Zheng Weihong, and R. R. P. Singh, Phys. Rev. Lett. **85**, 4373 (2000).
[43] Duality arguments show that P2 cannot be located in the region $J_\times > J$.